Real-time Discovery of AT2020xnd: A Fast, Luminous Ultraviolet Transient with Minimal Radioactive Ejecta

Daniel A. Perley,[1] Anna Y. Q. Ho,[2 3] Yuhan Yao,[4] Christo er Fremling,[4] Joseph P. Anderson,[5] Steve Schulze,[6] Harsh Kumar,[7 8] G. C. Anupama,[9] Sudhanshu Barway,[9] Eric C. Bellm,[10] Varun Bhalerao,[7] Ting-Wan Chen,[6] Dmitry A. Duev,[4] Lluís Galbany,[11] Matthew J. Graham,[4] Mariusz Gromadzki,[12] Claudia P. Gutiérrez,[13 14] Nada Ihanec,[12] Cosimo Inserra,[15] Mansi M. Kasliwal,[4] Erik C. Kool,[6] S. R. Kulkarni,[4] Russ R. Laher,[16] Frank J. Masci,[16] James D. Neill,[4] Matt Nicholl,[17] Miika Pursiainen,[18] Joannes van Roestel,[4] Yashvi Sharma,[4] Jesper Sollerman,[6] Richard Walters,[4] Philip Wiseman[19]

[1] *Astrophysics Research Institute, Liverpool John Moores University, IC2, Liverpool Science Park, 146 Brownlow Hill, Liverpool L3 5RF, UK*
[2] *Department of Astronomy, University of California, Berkeley, 94720, USA*
[3] *Miller Institute for Basic Research in Science, 468 Donner Lab, Berkeley, CA 94720, USA*
[4] *Division of Physics, Mathematics, and Astronomy, California Institute of Technology, Pasadena, CA 91125, USA*
[5] *European Southern Observatory, Alonso de Córdova 3107, Casilla 19 Santiago, Chile*
[6] *Department of Astronomy, The Oskar Klein Centre, Stockholm University, AlbaNova, 10691, Stockholm, Sweden*
[7] *Indian Institute of Technology Bombay, Powai, Mumbai 400076, India*
[8] *LSSTC DSFP Fellow*
[9] *Indian Institute of Astrophysics, II Block Koramangala, Bengaluru 560034, India*
[10] *DIRAC Institute, Department of Astronomy, University of Washington, 3910 15th Avenue NE, Seattle, WA 98195, USA*
[11] *Departamento de Física Teórica y del Cosmos, Universidad de Granada, E-18071 Granada, Spain.*
[12] *Astronomical Observatory, University of Warsaw, Al. Ujazdowskie 4, 00-478 Warsaw, Poland*
[13] *Finnish Centre for Astronomy with ESO (FINCA), FI-20014 University of Turku, Finland*
[14] *Tuorla Observatory, Department of Physics and Astronomy, FI-20014 University of Turku, Finland*
[15] *School of Physics & Astronomy, Cardi University, Queens Buildings, The Parade, Cardi CF24 3AA, UK*
[16] *IPAC, California Institute of Technology, 1200 E. California Blvd, Pasadena, CA 91125, USA*
[17] *Birmingham Institute for Gravitational Wave Astronomy and School of Physics and Astronomy, University of Birmingham, Birmingham B15 2TT, UK*
[18] *DTU Space, National Space Institute, Technical University of Denmark, Elektrovej 327, 2800 Kgs. Lyngby, Denmark*
[19] *School of Physics and Astronomy, University of Southampton, Southampton SO17 1BJ, UK*

Accepted XXX. Received YYY; in original form ZZZ

ABSTRACT

The many unusual properties of the enigmatic AT2018cow suggested that at least some subset of the empirical class of fast blue optical transients (FBOTs) represents a genuinely new astrophysical phenomenon. Unfortunately, the intrinsic rarity and eeting nature of these events have made it di cult to identify additional examples early enough to acquire the observations necessary to constrain theoretical models. We present here the Zwicky Transient Facility discovery of AT2020xnd (ZTF20acigmel, the Camel) at = 0 243, the rst unambiguous AT2018cow analog to be found and con rmed in real time. AT2018cow and AT2020xnd share all key observational properties: a fast optical rise, sustained high photospheric temperature, absence of a second peak attributable to ejection of a radioactively-heated stellar envelope, extremely luminous radio, millimetre, and X-ray emission, and a dwarf-galaxy host. This supports the argument that AT2018cow-like events represent a distinct phenomenon from slower-evolving radio-quiet supernovae, likely requiring a di erent progenitor or a di erent central engine. The sample properties of the four known members of this class to date disfavour tidal disruption models but are consistent with the alternative model of an accretion powered jet following the direct collapse of a massive star to a black hole. Contextual ltering of alert streams combined with rapid photometric veri cation using multi-band imaging provides an e cient way to identify future members of this class, even at high redshift.

Key words: transients: supernovae supernovae: individual: AT2020xnd

1 INTRODUCTION

A typical supernova rises on a timescale of days to weeks and fades away on a timescale of weeks to months (Villar et al. 2017;

E-mail: d.a.perley@ljmu.ac.uk

Perley et al. 2020). For stars that explode as supergiants, the rise timescale is governed by the cooling of the shock-heated photosphere and the fading timescale is governed by the gradual recombination of the ejecta (Arnett 1980; Weiler 2003; Zampieri 2017). For stars that explode in a compact state (stripped-envelope Wolf-Rayet stars and white dwarfs), the emission from the shock breakout and cooling is primarily at X-ray wavelengths and the rise and fall in the optical band are instead dominated by the dispersal of heat from newly-synthesized radioactive elements through the expanding ejecta (Arnett 1982).

Over the past decade, a population of transients with fast rise times (rise 1 7 days), fast decay times (decline 1•2 3 12 days), and a range of peak optical luminosities (16 ≳ peak ≳ 22) has been uncovered by wide-area surveys, with the largest samples originating from Pan-STARRS (PS1; Drout et al. 2014) and the Dark Energy Survey (DES; Pursiainen et al. 2018). These are sometimes called Rapidly Evolving Transients (RETs), Fast-Blue Optical Transients (FBOTs), or Fast-Evolving Luminous Transients (FELTs; Rest et al. 2018). Events with these properties simultaneously require an energetic shock, a large pre-explosion radius, and a low ejecta mass (Inserra 2019). While this combination of parameters is unusual it is not without precedent: type IIb supernovae, which are thought to originate from the explosion of a compact star with an extended but tenuous hydrogen atmosphere, show an initial early shock-breakout peak similar in nature to FBOTs (e.g. Fremling et al. 2019). However, the initial peak in type IIb SNe is not as luminous and it is followed by a second radioactively-powered peak of comparable optical luminosity that is not seen in FBOTs. The poorly-understood class of Type Ibn supernovae (Pastorello et al. 2007) also shows many similarities to the DES/PS1 FBOTs (Fox & Smith 2019).

The seminal event in the understanding of this class was the discovery of AT2018cow at 60 Mpc (Prentice et al. 2018). The rise to peak was very fast (≲3 days from explosion to peak), it was extremely luminous at peak, and it faded quickly properties characteristic of the PS1 and DES FBOTs. However, after peak it displayed a number of unexpected and indeed unprecedented behaviours: (a) the spectrum remained continuum-dominated throughout, with a high blackbody temperature (10000 K) and a photosphere that expanded rapidly before peak but then propagated inward (Perley et al. 2019); (b) it was extremely luminous at radio and millimetre wavelengths, with a millimetre light curve that did not reach maximum for several weeks (Ho et al. 2019); (c) it was also luminous at X-ray wavelengths, and showed an erratic light curve that ickered repeatedly up and down by a factor of ten in ux on timescales of days (Ho et al. 2019; Margutti et al. 2019; Kuin et al. 2019; Rivera Sandoval et al. 2018). Additionally, late-time spectra were dominated by intermediate-width lines of hydrogen and helium.

These properties impose several additional stringent requirements on the progenitor. The lack of a second peak implies that it did not produce a large amount of radioactive nickel or unbound ejecta (Perley et al. 2019). The high radio luminosity and late millimetre peak imply dense circumstellar material (CSM) beyond the optical photospheric radius (Ho et al. 2019). The rapid X-ray variability requires a compact and long-lived central engine (or perhaps a complex shock in a con ned structure) that is either exposed to the viewer or lightly screened (Margutti et al. 2019; Ho et al. 2019).

A variety of models have appeared in the literature attempting to explain this combination of properties. Electron-capture supernovae and fallback supernovae are commonly appealed to since both naturally explain the low ejecta mass, with either a proto-magnetar or an accretion-powered jet invoked to explain the fast rise and luminous X-ray/radio emission (Perley et al. 2019; Margutti et al. 2019; Quataert et al. 2019; Lyutikov & Toonen 2019; Piro & Lu 2020). However, many other models exist, including a range of models that associate AT2018cow with an unusual tidal disruption event (involving an intermediate-mass or even stellar-mass black hole) rather than an unusual supernova (Kuin et al. 2019; Perley et al. 2019; Liu et al. 2018; Uno & Maeda 2020; Kremer et al. 2020).

A challenge in distinguishing di erent models is the fact that only a single well-observed event exists (AT2018cow itself). While the data set for this event is excellent, it is unknown whether any of its qualitative or quantitative properties are essential to the phenomenon (as opposed to peculiar features of this event alone). It is plausible to assume that some of the DES and PS1 FBOTs represent the same generic phenomenon, but some members of these samples may be physically unrelated: for example, many exhibit a much lower peak luminosity or show evidence of cooling towards standard recombination temperatures, and no rm constraints exist on their behaviour outside the optical band. Thus, while the DES/PS1 samples are quite large and have been analyzed in some detail (Wiseman et al. 2020), the bulk sample properties cannot con dently be held to be indicative of the nature of AT2018cow. As a result there is no rm constraint on the cosmic rate, typical host-galaxy environment, or degree of internal diversity among other examples of this phenomenon.

Recently, two additional AT2018cow-like objects have been reported in the literature: CSS161010 (Coppejans et al. 2020) and ZTF18abvkwla (Koala , Ho et al. 2020b). Both of these events show very luminous radio emission lasting for months following the optical event; both also originated from dwarf galaxies (the host of ZTF18abvkwla is very strongly star-forming, that of CSS161010 much less so). Unfortunately, in neither case was the nature of the transient recognized early enough in its evolution to motivate a fast and deep optical campaign to establish the temperature evolution in detail[1] or an early X-ray campaign to search for rapid variability.

In this paper, we present the discovery of AT2020xnd (ZTF20acigmel, a.k.a. The Camel), a fast optical transient very similar to AT2018cow that was identi ed in real time using the Zwicky Transient Facility (ZTF; Bellm et al. 2019a; Graham et al. 2019) via our custom search pipeline. We outline our discovery process and present the deep optical follow-up observations that our early discovery enabled. We demonstrate that, like AT2018cow, this event showed no classical, radioactively-powered supernova, it remained very blue until late times, and it was extremely luminous across the electromagnetic spectrum. These properties suggest that the key features of AT2018cow are shared by other members of the class and indeed are likely the de ning aspects of the phenomenon, fundamentally separating AT2018cow and its ilk from other fast-rising transients. Our discovery also provides a road-map for gradually building up samples of well-observed events in the coming years using high-cadence surveys.

2 OBSERVATIONS

2.1 ZTF Discovery

ZTF is an optical time-domain facility conducting a series of transient surveys (Bellm et al. 2019b) using the 48-inch Oschin Schimdt Telescope at Palomar Observatory. These include a public survey in and (conducted at three-day cadence through September 2020 and two-day cadence from October 2020) and a one-day cadence

[1] Some optical follow-up of CSS161010 was acquired but the light curve is not yet published.

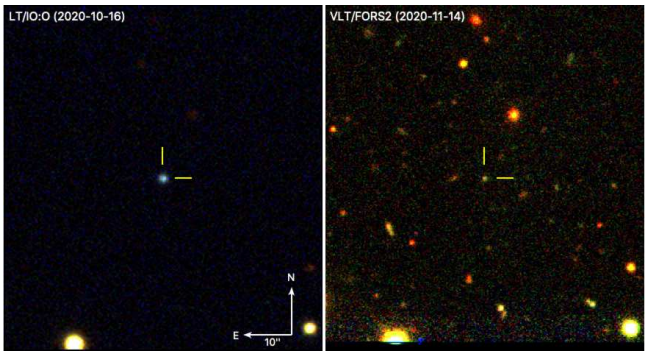

Figure 1. RGB false-colour / / image of the transient from the Liverpool Telescope 3 days after peak (left panel), compared to late-time VLT / / imaging 26 days after peak (right panel). The source is distinctly blue at early times. The host galaxy probably dominates the ux in the VLT measurement.

Caltech survey in and . The ZTF observing system is described in Dekany et al. (2020), and images are processed with the ZTF real-time reduction and image subtraction pipeline at the Infrared Processing & Analysis Center (Masci et al. 2019). Each 5- detection in a subtracted image is registered as an alert (Patterson et al. 2019), and each alert receives machine-learning based real-bogus scores, one based on a random-forest classi er (Mahabal et al. 2019) and one based on a neural network (Duev et al. 2019). The three nearest Pan-STARRS (Flewelling et al. 2020) sources receive a star-galaxy score to assist with identifying stellar vs. extragalactic transients (Tachibana & Miller 2018). The alert stream is distributed to a variety of community brokers; the one used for this paper was `kowalski`[2].

One of the primary goals of ZTF, particularly with the higher-cadence surveys, is to nd fast extragalactic transients such as gamma-ray burst afterglows and AT2018cow-like events. To this end, a lter has been set up with the following criteria:

A deep-learning based real-bogus score exceeding 0.65
At least two detections, with a duration between them exceeding 20 minutes
A Galactic latitude exceeding 15 deg
A criterion to remove artifacts from nearby bright stars (similar to that employed in Perley et al. 2020)
No coincident stellar counterpart (does not have a PS1 catalog match with a star-galaxy score exceeding 0.76 within 2 arcsec)
Detected at a magnitude brighter than 20 mag

The resulting candidates are then sorted into four groups:

1. New transients (those with no previous detections prior to the current night).
2. High-redshift transients (those with a DESI Legacy Imaging Survey DR8 (hereafter Legacy Survey ; Dey et al. 2019) counterpart within three arcseconds with a photometric redshift exceeding 0.4)
3. Fast-peaking transients: transients with a light curve that has peaked, i.e. has pre- and post-detections 1-sigma below peak, and where the time from half-max to max is under ve days, as per Ho et al. (2020b).
4. Fast-evolving transients: transients that rise more rapidly than 1 mag/day or fade more rapidly than 0.3 mag/day (see Andreoni et al. 2020).

[2] https://github.com/dmitryduev/kowalski

Every day, one of us (DAP, AYQH, YY) scans the resulting data stream, which usually has roughly 20 candidates. In addition, once per week forced photometry is run on all transients from the previous week, to identify candidates missed because of sub-threshold detections.

ZTF20acigmel passed the lter on 2020-10-12 under criterion 2 above: it is a new source coincident with a faint extended Legacy Survey source (type REX) with a high photometric redshift (= 1 33 $^{0\ 76}_{0\ 40}$; Zhou et al. 2021). It was not immediately identi ed as a transient of interest during scanning: the event was relatively faint (19 7 mag, 20 1 mag), and the most recent upper limit was three days prior and relatively shallow (20 2 mag). It was identi ed as a candidate again on 2020-10-14 following a slight rise in ux and also not saved. On 2020-10-16 it was agged a third time, and by this time it has faded signi cantly from the peak, suggesting fast evolution. It was saved as a candidate and registered to TNS, and the Liverpool Telescope (Steele et al. 2004) was triggered for follow-up observations. Follow-up observations were organized and coordinated using the GROWTH Marshal (Kasliwal et al. 2019).

After the transient had faded, we re-ran forced photometry for all observations of the eld using the average position for all measurements (J2000 coordinates =22:20:02.014, = 02:50:25.35). This photometry is given in Table 1.

2.2 LT Observations

We obtained imaging observations using the 2m robotic Liverpool Telescope (LT) on two successive nights (beginning at approximately 2020-10-17 00:07 UT and 2020-10-17 20:34 UT, respectively), using 60-second exposures in all ve Sloan Digital Sky Survey (SDSS) lters ( ). AT2020xnd was well-detected in all bands in both of these observations (Figure 1). (A longer observation was also obtained on 2020-10-20, although weather conditions were poor and only unconstraining upper limits were obtained.) The magnitude of the transient was measured in all images using basic aperture photometry (aperture radius 1.5), calibrated against SDSS secondary reference stars.

Comparison to the P48 observations con rmed a rapid drop in ux: by 0 5 0 1 mag over the 3 days between the epoch of apparent maximum light and the rst LT observation, then another 0 3 0 1 during just the next 20.5 hours (both measurements are in -band). The observed colour was very blue (= 0 42 0 05 mag in the rst LT epoch and = 0 52 0 10 mag in the second LT epoch, after correcting for Galactic reddening of = 0 07 mag; Schla y & Finkbeiner 2011). Blue colours are commonly observed in young supernovae and in cataclysmic variables, but both the degree of the colour and its persistence almost 1 mag into the decline are unusual. However, persistent blue colours after peak were a hallmark of AT2018cow (Perley et al. 2019). This, in combination with the Legacy Survey detection of a probable host galaxy, motivated additional follow-up, in particular spectroscopy (2.7).

2.3 P60 Observations

Additional imaging observations were acquired with the Rainbow Camera (RC) of the Spectral Energy Distribution Machine (SEDM) on the Palomar 60-inch telescope (Blagorodnova et al. 2018). Observations were taken using all four lters ( ) and reduced using the basic RC pipeline, and photometry was performed following the procedures of Fremling et al. (2016). Due to the fading of the source and limited sensitivity of the detector only upper limits were obtained

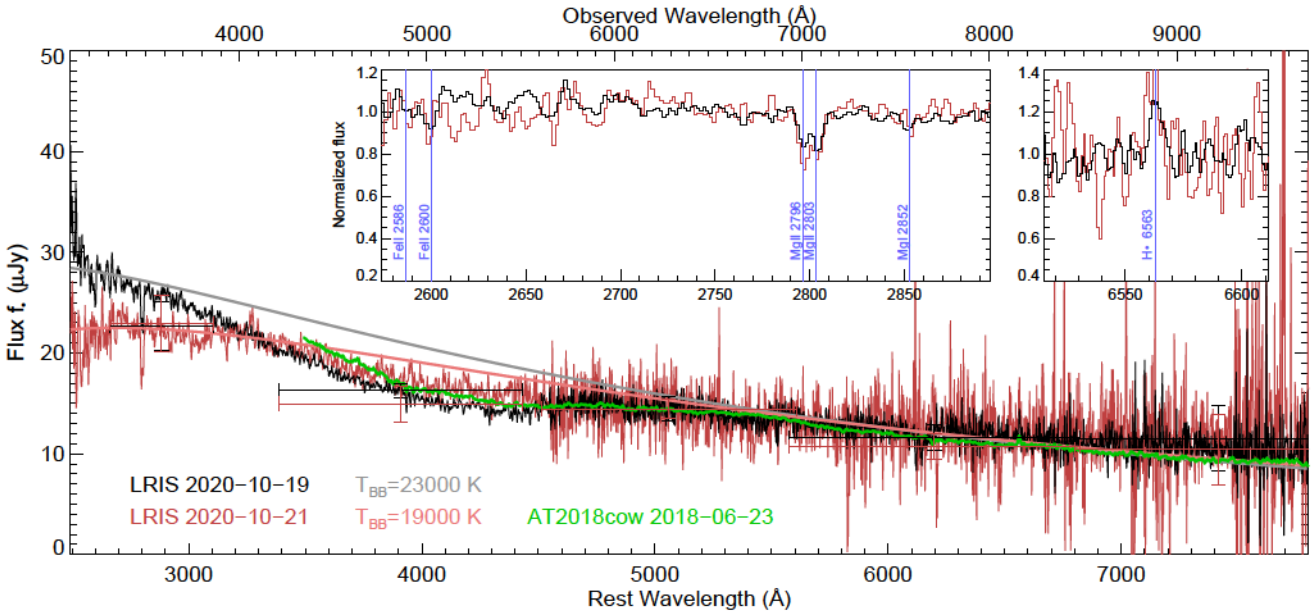

Figure 2. LRIS spectra of AT2020xnd, acquired two days apart and approximately one week after the peak of the optical light curve. The first spectrum is shown in black; the second spectrum is shown in red and has been rescaled in flux to match the first (in r-band). Theoretical blackbody spectra are also shown as thick curves, and a spectrum of AT2018cow at similar phase also plotted for comparison. Both spectra are featureless, although there is a hint of an extremely broad absorption feature centred around 4000Å (rest frame) in the first spectrum. The Mg II $\lambda\lambda$2796,2803 narrow absorption doublet is seen in both spectra along with possible low-significance detection of absorption lines of Mg I and Fe II (large inset), and weak emission from Hα (small inset).

in u-band, but detections confirming continued fading of the source were secured in all three remaining filters on 2020-10-20 and 2020-10-21. After that time, the event became too faint to secure useful detections with SEDM.

2.4 GIT Observations

On 2020-10-20 at 13:45 UT, we started imaging observations of AT2020xnd on the 0.7m GROWTH-India Telescope (GIT) located at the Indian Astronomical Observatory (IAO), Hanle-Ladakh (India). The data were acquired in r' band with multiple 300 sec exposures for four successive nights, although only an upper limit was obtained on 2020-10-23 due to poor observing conditions. Reduction was performed using the standard GIT pipeline. PSF photometry of the transient was performed with PS1 stars as a reference.

2.5 NTT Observations

Follow-up was provided using the ESO Faint Object Spectrograph and Camera (EFOSC2) on the 3.6m New Technology Telescope (NTT) at La Silla as part of the ePESSTO+ project (Smartt et al. 2015). Two epochs were acquired: the first on 2020-10-20 ($ugri$, under dark conditions) and the second on 2020-10-23 (g and r only, under bright conditions). A basic reduction of the data was performed using IDL, and photometry of AT2020xnd was performed using an aperture radius of 1.0 arcsec.

2.6 VLT Imaging Observations

We obtained several epochs of imaging using FORS2 on the Very Large Telescope at Paranal, Chile, under DDT proposal 106.21U2. Observations were obtained in the gri filters on UT 2020-11-03, 2020-11-04, 2020-11-05, 2020-11-09, 2020-11-14, and 2020-12-06. (Additionally, u-band observations were obtained on 2020-11-14.) An image of the field is shown in Figure 1. Reduction and photometry were performed using the same method as for the NTT observations. Because no image subtraction was performed, these measurements include (and at this epoch, are likely dominated by) the host galaxy.

2.7 Keck/LRIS Spectroscopy

We obtained spectroscopy of AT2020xnd using the Low-Resolution Imaging Spectrometer (LRIS; Oke et al. 1995) on the Keck I Telescope on 2020-10-19 and 2020-10-21. Observations were reduced using LPipe (Perley 2019). Both spectra (Figure 2) show a very hot, blue continuum with no easily-identifiable broad features.

A series of narrow absorption lines are superimposed on the continuum of both spectra. The strong Mg II $\lambda\lambda$2797,2801 doublet, redshifted to $z = 0.2433$, is prominent in both observations. Mg I λ2852 and Fe II λ2600 may also be present (at lower significance). These features establish $z = 0.2433$ as a minimum redshift. No other absorption lines are observed, although a weak, narrow emission line of Hα is also seen in both spectra at a consistent redshift, which if attributed to the host galaxy fixes this as the redshift of the transient. We will assume $z = 0.2433$ throughout this paper. (We assume a basic cosmology of $\Omega_M = 0.3$, $\Omega_\Lambda = 0.7$, $h = 0.7$; implying DM = 40.44 mag.)

The spectra show some deviation from a simple blackbody curve, with a slight depression in flux between approximately 3000-5000 Å in the rest frame. There is some uncertainty in the exact shape of the spectrum due to uncertain atmospheric corrections and wavelength-dependent slit losses as well as limited wavelength overlap between the blue and red arms of the spectrograph. However, the spectra and the close-to-simultaneous LT photometry self-consistently suggest a depression in flux in the vicinity of the observed g-band (rest-frame wavelengths between 3500-4500 Å), similar to what was observed

Table 1. Photometry of AT2020xnd.

MJD	Instrument	lter	mag	unc.	ABmag
59134.17188	P48+ZTF		20.52	0.16	20.34
59134.18359	P48+ZTF		20.08	0.09	19.90
59134.22656	P48+ZTF		19.68	0.06	19.43
59134.22656	P48+ZTF		19.69	0.07	19.43
59135.26953	P48+ZTF		19.74	0.07	19.56
59136.17578	P48+ZTF		19.87	0.09	19.70
59136.21094	P48+ZTF		19.49	0.05	19.23
59136.21484	P48+ZTF		19.51	0.05	19.26
59138.13281	P48+ZTF		19.92	0.10	19.74
59138.19531	P48+ZTF		20.00	0.09	19.74
59138.19531	P48+ZTF		20.07	0.10	19.81
59139.19141	P48+ZTF		20.07	0.09	19.82
59140.16797	P48+ZTF		20.66	0.13	20.41
59140.17969	P48+ZTF		20.53	0.11	20.28
59140.23047	P48+ZTF		20.78	0.16	20.60
59141.17188	P48+ZTF		20.91	0.28	20.74
59142.14453	P48+ZTF		21.01	0.19	20.83
59142.14453	P48+ZTF		21.14	0.23	20.97
59143.20703	P48+ZTF		21.31	0.23	21.06
59143.22656	P48+ZTF		21.48	0.27	21.30
59139.00391	LT+IOO		20.20	0.02	19.95
59139.00781	LT+IOO		20.25	0.04	20.07
59139.00781	LT+IOO		20.44	0.05	20.31
59139.00781	LT+IOO		20.44	0.14	20.32
59139.01172	LT+IOO		19.87	0.05	19.58
59139.85938	LT+IOO		20.51	0.07	20.26
59139.85938	LT+IOO		20.47	0.04	20.29
59139.85938	LT+IOO		20.75	0.07	20.62
59139.86328	LT+IOO		20.77	0.21	20.65
59139.86328	LT+IOO		20.08	0.07	19.79
59142.62891	GIT		21.52	0.06	21.35
59143.70703	GIT		21.69	0.06	21.52
59145.67578	GIT		22.11	0.07	21.93
59144.41406	Swift+UVOT		20.35	0.25	21.03
59151.46875	Swift+UVOT	1	21.64	0.36	22.70
59142.09375	P60+SEDM		20.95	0.14	20.77
59142.09766	P60+SEDM		21.04	0.09	20.79
59143.10156	P60+SEDM		21.29	0.14	21.11
59143.10547	P60+SEDM		21.60	0.12	21.35
59143.10938	P60+SEDM		21.32	0.20	21.19
59145.06641	NTT+EFOSC2		21.60	0.07	21.31
59145.07422	NTT+EFOSC2		21.83	0.03	21.58
59145.08203	NTT+EFOSC2		21.95	0.04	21.77
59145.09375	NTT+EFOSC2		22.08	0.06	21.95
59147.03906	NTT+EFOSC2		22.31	0.11	22.13
59147.06250	NTT+EFOSC2		22.29	0.07	22.04
59156.03125	VLT+FORS2		23.47	0.05	23.22
59156.04297	VLT+FORS2		23.41	0.05	23.23
59156.05078	VLT+FORS2		23.41	0.05	23.28
59157.02734	VLT+FORS2		23.67	0.03	23.42
59157.03906	VLT+FORS2		23.53	0.05	23.35
59157.05078	VLT+FORS2		23.76	0.07	23.63
59158.07812	VLT+FORS2		23.81	0.05	23.56
59158.07812	VLT+FORS2		23.62	0.04	23.44
59158.08984	VLT+FORS2		23.65	0.09	23.52
59162.06250	VLT+FORS2		24.02	0.03	23.77
59162.07422	VLT+FORS2		23.81	0.05	23.63
59162.08594	VLT+FORS2		23.75	0.07	23.62
59167.02344	VLT+FORS2		24.71	0.16	24.42
59167.04297	VLT+FORS2		24.39	0.12	24.14
59167.05078	VLT+FORS2		23.99	0.10	23.81
59167.05469	VLT+FORS2		23.73	0.14	23.60
59189.02734	VLT+FORS2		25.07	0.18	24.82
59189.03906	VLT+FORS2		24.51	0.14	24.33
59189.04297	VLT+FORS2		23.81	0.14	23.68

In standard reference system for the lter; not corrected for extinction. Corrected for Galactic extinction.

in spectra of AT2018cow at similar phases after peak (Perley et al. 2019). A spectrum of AT2018cow at a similar phase (from the Discovery Channel Telescope about six days after the peak; the ux has been rescaled) is shown for comparison in Figure 2.

2.8 Multiwavelength Observations

After the con rmation of AT2020xnd as an extragalactic, fast-evolving transient we also obtained extensive observations at radio and millimetre wavelengths, and a series of X-ray observations were also acquired using the Swift X-Ray Telescope (XRT) and the Chandra X-ray Telescope. (Swift simultaneously acquired Ultraviolet-Optical Telescope (UVOT) observations, which secured only marginal detections of the transient.) The transient is luminous at radio, millimeter, and X-ray wavelengths (Ho et al. 2020a; Matthews et al. 2020), further con rming its similarity to AT2018cow. The inferred properties of the forward shock will be presented in separate work by Ho et al.

3 ANALYSIS AND DISCUSSION

3.1 A Fast-Peaking Optical Transient

The optical light curve of 2020xnd is plotted in Figure 3. Overplotted for reference as solid lines is the light curve of AT2018cow, interpolated as in Perley et al. (2019). Colours are matched approximately by rest-frame lter bandpass (for AT2018cow we plot UVW1, u, g, and r to match the colours of u, g, r, and i, respectively). No o sets have been applied, although the reference time ($_0$ at MJD 59132.0) was chosen for the best match to AT2018cow.

While there is some uncertainty regarding the exact time of the peak and the nature of the rise (due to limited sampling and non-negligible photometric errors), the light curves are strikingly similar. The peak absolute AB magnitude ( ) of AT 2020xnd is approximately $_{5000}$ = 20 4 or $_{3900}$ = 20 7. The total time above half peak is about 6 days as observed (two days to rise from half-peak, then four days to decay an equivalent amount) or 5 days in the rest-frame. These values are quite similar to those inferred for AT2018cow ($_{4600}$ = 20 4, $_{1\bullet2}$ 4 5d; Perley et al. 2019), and quite unlike nearly all other transients found by ZTF to date (Perley et al. 2020).

3.2 A Persistently Blue, Hot Transient

The spectrum and spectral energy distribution (SED) of AT2020xnd imply a hot photosphere peaking well into the ultraviolet that persists throughout the observed evolution of the transient. In Figure 2 we show both epochs of spectroscopy and SEDs from two (close in time) epochs of Liverpool Telescope photometry.

We t the multiband photometry from the rst two LT epochs (at = 7 01 and = 7 86 observer-frame days after $_0$) and the rst NTT epoch (at = 13 08 days) to a simple blackbody model. The e ective temperature across all three epochs is very high (= 20000 2000) and does not evolve between the rst and last epochs to within the uncertainties. The e ective blackbody radius moves inward, from = 80 30 AU at 7 days to = 39 5 AU at 13 days.[3]

These are similar values to AT2018cow at equivalent times (Perley et al. 2019) and the physical implications are also similar: the photosphere is inconsistent with a dense sphere of expanding

[3] Since the host extinction is unknown, these are technically lower limits on the temperature and upper limits on the radius.

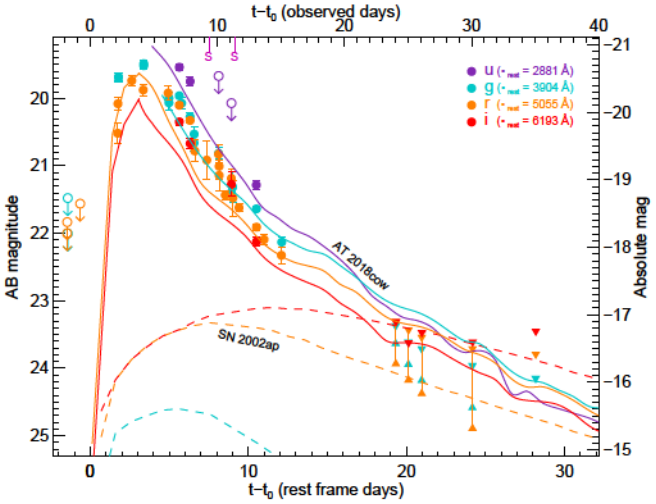

Figure 3. Optical (observer-frame $ugri$) light curve of AT2020xnd (data points), compared with rest-frame equivalent light curves of AT2018cow (solid curves, based on the interpolation in Perley et al. 2019) and the low-luminosity SN Ic-BL SN2002ap (dashed curve; from Mazzali et al. 2002). All measurements have been corrected for Galactic extinction. The 'S' marks denote the epochs of the two spectra shown in Figure 2.

ejecta such as that seen in ordinary supernovae. While a recessing photosphere can occur within an expanding explosion if the opacity drops quickly enough, it would be surprising for this to happen in material that remains far above the recombination temperature at small radii. (We would also expect to observe strong emission lines during this transition.) We conclude that, as was the case for AT2018cow, the emission from AT2020xnd originates from an entirely different component, such as a confined ejecta torus close to the central engine or dense shell of pre-existing material.

3.3 No Evidence For A Radioactively-Powered Supernova

The successful explosion of a massive star is expected to produce a large amount of hot, dense, freely-expanding ejecta. In the previous section, we argue that such a component cannot reproduce the early-time evolution of AT2020xnd. However, if AT2020xnd originates from a star that successfully exploded, we might still expect to see the ejecta at later times once this lower-luminosity component is no longer outshined by the hot blue component.

Analysis of the late-time behaviour of this transient is complicated by the presence of the host galaxy, which is of comparable luminosity to the transient during our late observations with the VLT and NTT. The galaxy is marginally detected in the Legacy Survey with quoted magnitudes of $g = 24.85^{-0.34}_{+0.52}$, $r = 24.08^{-0.40}_{+0.65}$, $z = 23.96^{-0.60}_{+1.47}$ (2σ uncertainties). The Legacy Survey images are much shallower than our late-time VLT images, so they are not useful for subtracting the host galaxy flux from those observations.

To constrain the late-time flux of the transient, we assume two different extreme scenarios to bracket the possible evolution. To produce upper limits on the late-time flux, we assume all of the measured flux originates from the transient, and place a downward-pointing triangle on Figure 3 at 2σ above the measurement. To produce a lower limit, we assume a maximum allowed host-galaxy flux of 2σ above the final VLT measurement, and subtract this from all previous measurements. This is plotted as an upward-pointing arrow.

The maximum luminosity of any supernova component in AT2020xnd at $t \sim 30$ days is -16.5 AB mag ($\nu L_\nu \sim 10^{42}$ erg/s). This is comparable to the underluminous Type Ic 2002ap (Foley et al. 2003; Mazzali et al. 2002), which is shown for reference in Figure 3), or to low-luminosity Type II SNe. This limit is very conservative—not only does it neglect the (probably substantial) contribution of the host galaxy but it also does not take into account the continued presence of the blue component, which will also still be contributing to (and probably dominating) the emission at these times. A late-time host-galaxy measurement will be required to put tight limits on SN-like emission from this transient, but we can clearly rule out a bright supernova component and suggest that even a low-luminosity one is quite unlikely. This implies that, if the progenitor is a massive star, it either expelled very little material or produced minimal radioactive nickel. Low-luminosity Ib/c and SN II have characteristic nickel masses of between 10^{-2} to 10^{-1} $M_\odot$ (Müller et al. 2017): assuming a similar degree of radiation trapping in the slow ejecta, the amount synthesised and expelled by AT2020xnd must have been significantly less than this. The $M_{R,\mathrm{peak}} - M(56\mathrm{Ni})$ relation of Dessart et al. (2016) would imply a limit of $M(^{56}\mathrm{Ni}) < 0.02 M_\odot$.

Extremely low-luminosity (and nickel-poor) supernovae are not unprecedented (Hamuy 2003; Pastorello et al. 2004). However, it is notable that such a nickel-poor event is occurring alongside one of the most energetic radio transients known (Ho et al. 2021, in prep). Known radio-luminous transients associated with the deaths of massive stars are without exception accompanied by quite energetic supernovae (Weiler et al. 2002). This could suggest that the transient is not powered by a massive star at all (a possibility at odds with the dwarf star-forming nature of the host population; see next section), or that failure of the accompanying supernova is intrinsic to the phenomenon.

3.4 A Dwarf Host Galaxy With Modest Star-Formation

While a sizeable population of photometrically-identified fast-luminous transients exists and has now been subject to detailed sample analysis (Pursiainen et al. 2018; Wiseman et al. 2020), it is not yet clear how many of these are true AT2018cow-like events versus other fast phenomena (such as classical Type Ibn SNe, or "ordinary" SN types with luminous shock-cooling peaks whose secondary rise was missed). The sample of confirmed AT2018cow-like transients remains very small, although all three events published to date were localized to star-forming dwarf galaxies (Perley et al. 2020; Ho et al. 2020b; Coppejans et al. 2020) and this appears to be true of the broader (spectroscopically-unconfirmed) fast-luminous transient population from DES as well (Wiseman et al. 2020).

AT2020xnd continues this trend. There is insufficient data to fit an SED model to the host photometry (only three low-S/N detections from the Legacy Survey are available), although the optical luminosity (absolute magnitude -16.2) is consistent with a stellar mass between $3 \times 10^7 M_\odot$ and $3 \times 10^8 M_\odot$ (Blanton et al. 2011) and typical of galaxies with stellar mass of $\sim 10^8$ $M_\odot$, similar to the Small Magellanic Cloud. The star-formation rate is low: assuming that the weak emission feature seen in our LRIS spectra is indeed Hα emission from the galaxy (and assuming no host extinction), we measure a star-formation rate of SFR $= 0.020 \pm 0.005 M_\odot$ yr^{-1}, which is fairly characteristic of SN host galaxies of this mass at low redshift (Taggart & Perley 2019).

These observations continue to build the case that AT2018cow-like transients occur primarily (perhaps, exclusively) in dwarf galaxies, similar to superluminous supernovae and long-duration gamma-ray bursts. The modest specific star formation rate suggests that an extremely young population age or high volumetric star-formation rate

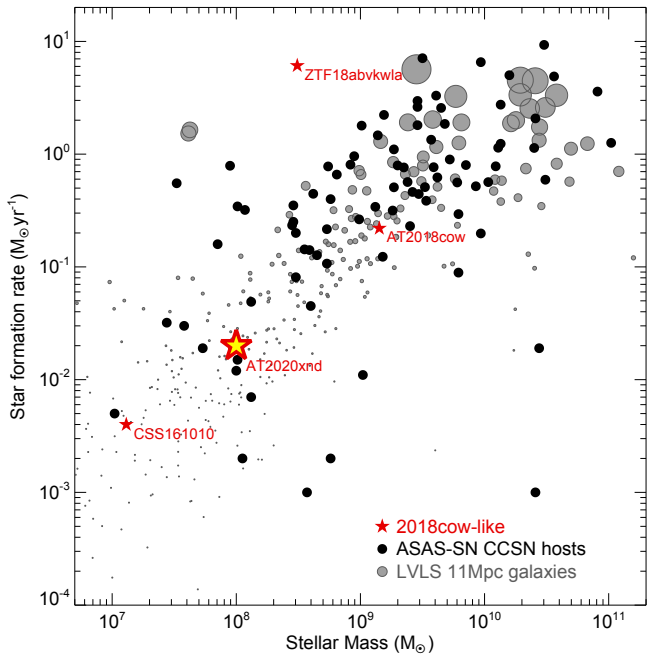

Figure 4. Estimates of the mass and star-formation rate of the host galaxy of AT2020xnd (star), compared to other hosts of AT2018cow-like events: AT2018cow itself, ZTF18abvkwla, and CSS161010 (Perley et al. 2019; Ho et al. 2019; Coppejans et al. 2020). To date there are no high-mass hosts, and three out of four have typical star-formation rates given their stellar mass. The core-collapse host galaxy sample of Taggart & Perley (2019) and galaxies within 11 Mpc from the Local Volume Legacy Survey (LVLS; Lee et al. 2011) are also shown for comparison (in black and in grey, respectively). LVLS symbol sizes are weighted by SFR for better visual comparison to the SFR-selected SN samples.

density is *not* a precondition, which disfavours (although does not rule out) models that require a modi ed IMF or extensive dynamical interactions, e ects expected only in the most extreme star-forming environments such as proto-globular clusters. The basic physical properties of the host galaxies for the four AT2018cow-like events with con rmed luminous radio emission are shown in Figure 4. While all four are low-mass galaxies, only ZTF18abkwla has been shown to be forming stars at an elevated rate. Recently-published IFU spectroscopy and millimetre observations of the host of AT2018cow (Lyman et al. 2020; Morokuma-Matsui et al. 2019) likewise argue against the notion of an elevated stellar or star-formation-rate density being essential for the production of the progenitor of this class.

4 CONCLUSIONS

We report the discovery and early characterization of AT 2020xnd, a fast-luminous optical transient at = 0 2433. The transient shares all key properties with AT2018cow: fast rise, high peak luminosity, featureless thermal spectrum, persistent blue colour throughout the decay, luminous radio emission, and a low-mass host galaxy whose star-formation rate is not particularly elevated. Its spectrum may contain high-velocity photospheric features at early times, although we do not know whether it showed narrow emission components at late times.

These observations suggest that the peculiar properties of AT2018cow are in fact typical of a new class of fast, energetic transients. They also reveal a sharp distinction between these events and others that occupy the same general region of luminosity-duration phase space (Perley et al. 2020): for example Type Ibn supernovae and shock-cooling emission from Type IIb supernovae, whose optical properties are somewhat less extreme and do not produce luminous radio emission. Understanding the nature of this mysterious class of AT2018cow-like astrophysical transients will require an integrative model that explains all of their key features: in particular, the strong contrast between an energetic high-velocity shock with the absence of a nickel-powered supernova.

An updated discussion of progenitor models in the complete context of the optical, radio, and X-ray data of this event will be deferred for upcoming work by Ho et al. For now, however, qualitative arguments seem to point towards a variant of the failed-supernova scenario rst proposed by Perley et al. (2019), in which the transient is produced by a jet driven by fallback accretion onto a black hole. The association with low-mass but otherwise typical star-forming galaxies argues for a massive stellar origin (and against alternative models involving tidal disruption of a star around a pre-existing intermediate-mass black hole), and the absence of a classical SN counterpart implies that most of the star s mass was not ejected. The hydrogen- and helium-rich late-time spectra of AT2018cow also support this model, although observations of this type could not be obtained for AT2020xnd.

If this model is correct, we should continue to observe the key features of AT2018cow and AT2020xnd in further members of this newly-recognized class of events. Our observations demonstrate an e ective method for rapidly identifying new candidates in the future. A rapid rise to ux well above that of its host galaxy, followed by immediate fading, is an identifying feature although as this property is shared with cataclysmic variables additional criteria are necessary. Angular extension of the candidate host in deep imaging surveys can provide an e ective means of eliminating the majority of Galactic cataclysmic variables from consideration, with multi-band photometric follow-up with 1 2 meter class telescopes immediately after peak providing a useful additional screening method to rapidly vet candidates for spectroscopy.

Even more robust ltering of false positives would be possible if reliable multi-colour host photometric redshifts, or even spectroscopic redshifts, of intermediate-redshift faint galaxies were widely available across most of the sky. While the apparently high-redshift nature of its host galaxy (as given by the Legacy Survey) allowed AT2020xnd to pass our lter, this was in some ways a coincidence: the true redshift was lower than the (wide) constraint provided by the 3-band Legacy Survey. Fortunately, over the coming decade the redshift completeness is poised to rapidly increase, with several large galaxy surveys in preparation including DESI, 4MOST, VLT/MOONS, and Rubin/LSST. When combined with future high-cadence wide- eld surveys similar to ZTF, this will allow far more robust redshift/luminosity-based ltering than is currently possible while also permitting candidates to be identi ed and followed up even more rapidly.

ACKNOWLEDGEMENTS

Based on observations obtained with the Samuel Oschin Telescope 48-inch and the 60-inch Telescope at the Palomar Observatory as part of the Zwicky Transient Facility project. ZTF is supported by the National Science Foundation under Grant No. AST-2034437 and a collaboration including Caltech, IPAC, the Weizmann Institute for Science, the Oskar Klein Centre at Stockholm University, the University of Maryland, Deutsches Elektronen-Synchrotron and Humboldt

University, the TANGO Consortium of Taiwan, the University of Wisconsin at Milwaukee, Trinity College Dublin, Lawrence Livermore National Laboratories, and IN2P3, France. Operations are conducted by COO, IPAC, and UW. The Liverpool Telescope is operated on the island of La Palma by Liverpool John Moores University in the Spanish Observatorio del Roque de los Muchachos of the Instituto de Astro sica de Canarias with nancial support from the UK Science and Technology Facilities Council. The SED Machine is based upon work supported by the National Science Foundation under Grant No. 1106171. Based on observations collected at the European Organisation for Astronomical Research in the Southern Hemisphere under ESO programme(s) 106.21U2 and 106.216C. We thank Stephane Blondin for helpful comments.

This work was supported by the GROWTH (Global Relay of Observatories Watching Transients Happen) project funded by the NSF under PIRE grant 1545949. GROWTH is a collaborative project among California Institute of Technology (USA), University of Maryland College Park (USA), University of Wisconsin Milwaukee (USA), Texas Tech University (USA), San Diego State University (USA), University of Washington (USA), Los Alamos National Laboratory (USA), Tokyo Institute of Technology (Japan), National Central University (Taiwan), Indian Institute of Astrophysics (India), Indian Institute of Technology Bombay (India), Weizmann Institute of Science (Israel), The Oskar Klein Centre at Stockholm University (Sweden), Humboldt University (Germany), Liverpool John Moores University (UK), and University of Sydney (Australia).

The GROWTH India telescope is a 70-cm telescope with a 0.7 degree eld of view, set up by the Indian Institute of Astrophysics and the Indian Institute of Technology Bombay with support from the Indo-US Science and Technology Forum (IUSSTF) and the Science and Engineering Research Board (SERB) of the Department of Science and Technology (DST), Government of India. It is located at the Indian Astronomical Observatory (Hanle), operated by the Indian Institute of Astrophysics (IIA). GROWTH-India project is supported by SERB and administered by IUSSTF.

Funding for the SDSS and SDSS-II has been provided by the Alfred P. Sloan Foundation, the Participating Institutions, the NSF, the U.S. Department of Energy, the National Aeronautics and Space Administration (NASA), the Japanese Monbukagakusho, the Max Planck Society, and the Higher Education Funding Council for England. The SDSS is managed by the Astrophysical Research Consortium for the Participating Institutions. The Participating Institutions are the American Museum of Natural History, Astrophysical Institute Potsdam, University of Basel, University of Cambridge, Case Western Reserve University, University of Chicago, Drexel University, Fermilab, the Institute for Advanced Study, the Japan Participation Group, Johns Hopkins University, the Joint Institute for Nuclear Astrophysics, the Kavli Institute for Particle Astrophysics and Cosmology, the Korean Scientist Group, the Chinese Academy of Sciences (LAMOST), Los Alamos National Laboratory, the Max-Planck-Institute for Astronomy (MPIA), the Max-Planck-Institute for Astrophysics (MPA), New Mexico State University, Ohio State University, University of Pittsburgh, University of Portsmouth, Princeton University, the United States Naval Observatory, and the University of Washington.

The Pan-STARRS1 Surveys (PS1) have been made possible through contributions of the Institute for Astronomy, the University of Hawaii, the Pan-STARRS Project O ce, the Max-Planck Society and its participating institutes, the Max Planck Institute for Astronomy, Heidelberg and the Max Planck Institute for Extraterrestrial Physics, Garching, The Johns Hopkins University, Durham University, the University of Edinburgh, Queen s University Belfast, the Harvard-Smithsonian Center for Astrophysics, the Las Cumbres Observatory Global Telescope Network Incorporated, the National Central University of Taiwan, the Space Telescope Science Institute, NASA under grant NNX08AR22G issued through the Planetary Science Division of the NASA Science Mission Directorate, the NSF under grant AST-1238877, the University of Maryland, and Eotvos Lorand University (ELTE).

The Legacy Surveys consist of three individual and complementary projects: the Dark Energy Camera Legacy Survey (DECaLS; NSF s OIR Lab Proposal ID 2014B-0404; PIs: David Schlegel and Arjun Dey), the Be ing-Arizona Sky Survey (BASS; NSF s OIR Lab Proposal ID 2015A-0801; PIs: Zhou Xu and Xiaohui Fan), and the Mayall z-band Legacy Survey (MzLS; NSF s OIR Lab Proposal ID 2016A-0453; PI: Arjun Dey). DECaLS, BASS and MzLS together include data obtained, respectively, at the Blanco telescope, Cerro Tololo Inter-American Observatory, The NSF s National Optical-Infrared Astronomy Research Laboratory (NSF s OIR Lab); the Bok telescope, Steward Observatory, University of Arizona; and the Mayall telescope, Kitt Peak National Observatory, NSF s OIR Lab. The Legacy Surveys project is honored to be permitted to conduct astronomical research on Iolkam Du ag (Kitt Peak), a mountain with particular signi cance to the Tohono O odham Nation.

This project used data obtained with the Dark Energy Camera (DECam), which was constructed by the Dark Energy Survey (DES) collaboration. Funding for the DES Projects has been provided by the U.S. Department of Energy, the U.S. National Science Foundation, the Ministry of Science and Education of Spain, the Science and Technology Facilities Council of the United Kingdom, the Higher Education Funding Council for England, the National Center for Supercomputing Applications at the University of Illinois at Urbana-Champaign, the Kavli Institute of Cosmological Physics at the University of Chicago, Center for Cosmology and Astro-Particle Physics at the Ohio State University, the Mitchell Institute for Fundamental Physics and Astronomy at Texas A&M University, Financiadora de Estudos e Projetos, Fundacao Carlos Chagas Filho de Amparo, Financiadora de Estudos e Projetos, Fundacao Carlos Chagas Filho de Amparo a Pesquisa do Estado do Rio de Janeiro, Conselho Nacional de Desenvolvimento Cienti co e Tecnologico and the Ministerio da Ciencia, Tecnologia e Inovacao, the Deutsche Forschungsgemeinschaft and the Collaborating Institutions in the Dark Energy Survey. The Collaborating Institutions are Argonne National Laboratory, the University of California at Santa Cruz, the University of Cambridge, Centro de Investigaciones Energeticas, Medioambientales y Tecnologicas-Madrid, the University of Chicago, University College London, the DES-Brazil Consortium, the University of Edinburgh, the Eidgenossische Technische Hochschule (ETH) Zurich, Fermi National Accelerator Laboratory, the University of Illinois at Urbana-Champaign, the Institut de Ciencies de l Espai (IEEC/CSIC), the Institut de Fisica d Altes Energies, Lawrence Berkeley National Laboratory, the Ludwig-Maximilians Universitat Munchen and the associated Excellence Cluster Universe, the University of Michigan, the National Optical Astronomy Observatory, the University of Nottingham, the Ohio State University, the University of Pennsylvania, the University of Portsmouth, SLAC National Accelerator Laboratory, Stanford University, the University of Sussex, and Texas A&M University.

The Legacy Surveys imaging of the DESI footprint is supported by the Director, O ce of Science, O ce of High Energy Physics of the U.S. Department of Energy under Contract No. DE-AC02-05CH1123, by the National Energy Research Scienti c Computing Center, a DOE O ce of Science User Facility under the same contract; and by the U.S. National Science Foundation, Division of Astronomical Sciences under Contract No. AST-0950945 to NOAO.

L.G. was funded by the European Union s Horizon 2020 research and innovation programme under the Marie Sk odowska-Curie grant agreement No. 839090. This work has been partially supported by the Spanish grant PGC2018-095317-B-C21 within the European Funds for Regional Development (FEDER). H.K. thanks the LSSTC Data Science Fellowship Program, which is funded by LSSTC, NSF Cybertraining Grant #1829740, the Brinson Foundation, and the Moore Foundation; his participation in the program has bene ted this work. E.C.K. acknowledges support from the G.R.E.A.T research environment funded by *Vetenskapsrådet*, the Swedish Research Council, under project number 2016-06012, and support from The Wenner-Gren Foundations. M.N. is supported by a Royal Astronomical Society Research Fellowship. M.G. is supported by the Polish NCN MAESTRO grant 2014/14/A/ST9/00121. T.-W.C. acknowledges the EU Funding under Marie Sk odowska-Curie grant H2020-MSCA-IF-2018-842471.

This research has made use of the NASA/IPAC Extragalactic Database (NED), which is operated by the Jet Propulsion Laboratory, California Institute of Technology, under contract with NASA. This research has made use of the VizieR catalogue access tool, CDS, Strasbourg, France (DOI : 10.26093/cds/vizier). The original description of the VizieR service was published in A&AS 143, 23.

Some of the data that contributed to this paper were obtained at the W. M. Keck Observatory, which is operated as a scienti c partnership among the California Institute of Technology, the University of California, and NASA. The Observatory was made possible by the generous nancial support of the W. M. Keck Foundation. The authors wish to recognize and acknowledge the very signi cant cultural role and reverence that the summit of Maunakea has always had within the indigenous Hawaiian community.

DATA AVAILABILITY

Photometry is provided in Table 1. Reduced LRIS spectra will be uploaded to WISErep. All P48, Liverpool Telescope, Swift, Keck, NTT, and VLT observations will be available online via their respective telescope archives.

REFERENCES

Andreoni I., et al., 2020, ApJ, 904, 155
Arnett W. D., 1980, ApJ, 237, 541
Arnett W. D., 1982, ApJ, 253, 785
Bellm E. C., et al., 2019a, PASP, 131, 018002
Bellm E. C., et al., 2019b, PASP, 131, 068003
Blagorodnova N., et al., 2018, PASP, 130, 035003
Blanton M. R., Kazin E., Muna D., Weaver B. A., Price-Whelan A., 2011, AJ, 142, 31
Coppejans D. L., et al., 2020, ApJ, 895, L23
Dekany R., et al., 2020, PASP, 132, 038001
Dessart L., Hillier D. J., Woosley S., Livne E., Waldman R., Yoon S.-C., Langer N., 2016, MNRAS, 458, 1618
Dey A., et al., 2019, AJ, 157, 168
Drout M. R., et al., 2014, ApJ, 794, 23
Duev D. A., et al., 2019, MNRAS, 489, 3582
Flewelling H. A., et al., 2020, ApJS, 251, 7
Foley R. J., et al., 2003, PASP, 115, 1220
Fox O. D., Smith N., 2019, MNRAS, 488, 3772
Fremling C., et al., 2016, A&A, 593, A68
Fremling C., et al., 2019, ApJ, 878, L5
Graham M. J., et al., 2019, PASP, 131, 078001
Hamuy M., 2003, ApJ, 582, 905
Ho A. Y. Q., et al., 2019, ApJ, 871, 73
Ho A. Y. Q., Perley D. A., Yao Y., 2020a, Transient Name Server AstroNote, 204, 1
Ho A. Y. Q., et al., 2020b, ApJ, 895, 49
Inserra C., 2019, Nature Astronomy, 3, 697
Kasliwal M. M., et al., 2019, PASP, 131, 038003
Kremer K., Lu W., Piro A. L., Chatterjee S., Rasio F. A., Ye C. S., 2020, arXiv e-prints, p. arXiv:2012.02796
Kuin N. P. M., et al., 2019, MNRAS, 487, 2505
Lee J. C., et al., 2011, ApJS, 192, 6
Liu L.-D., Zhang B., Wang L.-J., Dai Z.-G., 2018, ApJ, 868, L24
Lyman J. D., Galbany L., Sánchez S. F., Anderson J. P., Kuncarayakti H., Prieto J. L., 2020, MNRAS, 495, 992
Lyutikov M., Toonen S., 2019, MNRAS, 487, 5618
Mahabal A., et al., 2019, PASP, 131, 038002
Margutti R., et al., 2019, ApJ, 872, 18
Masci F. J., et al., 2019, PASP, 131, 018003
Matthews D., et al., 2020, Transient Name Server AstroNote, 218, 1
Mazzali P. A., et al., 2002, ApJ, 572, L61
Morokuma-Matsui K., et al., 2019, ApJ, 879, L13
Müller T., Prieto J. L., Pejcha O., Clocchiatti A., 2017, ApJ, 841, 127
Oke J. B., et al., 1995, PASP, 107, 375
Pastorello A., et al., 2004, MNRAS, 347, 74
Pastorello A., et al., 2007, Nature, 447, 829
Patterson M. T., et al., 2019, PASP, 131, 018001
Perley D. A., 2019, PASP, 131, 084503
Perley D. A., et al., 2019, MNRAS, 484, 1031
Perley D. A., et al., 2020, ApJ, 904, 35
Piro A. L., Lu W., 2020, ApJ, 894, 2
Prentice S. J., et al., 2018, ApJ, 865, L3
Pursiainen M., et al., 2018, MNRAS, 481, 894
Quataert E., Lecoanet D., Coughlin E. R., 2019, MNRAS, 485, L83
Rest A., et al., 2018, Nature Astronomy, 2, 307
Rivera Sandoval L. E., Maccarone T. J., Corsi A., Brown P. J., Pooley D., Wheeler J. C., 2018, MNRAS, 480, L146
Schla y E. F., Finkbeiner D. P., 2011, ApJ, 737, 103
Smartt S. J., et al., 2015, A&A, 579, A40
Steele I. A., et al., 2004, in Oschmann Jr. J. M., ed., Proc. SPIEVol. 5489, Ground-based Telescopes. pp 679 692, doi:10.1117/12.551456
Tachibana Y., Miller A. A., 2018, PASP, 130, 128001
Taggart K., Perley D., 2019, MNRAS accepted, p. arXiv:1911.09112
Uno K., Maeda K., 2020, ApJ, 905, L5
Villar V. A., Berger E., Metzger B. D., Guillochon J., 2017, ApJ, 849, 70
Weiler K., 2003, Supernovae and Gamma-Ray Bursters. Vol. 598, Springer, doi:10.1007/3-540-45863-8
Weiler K. W., Panagia N., Montes M. J., Sramek R. A., 2002, ARA&A, 40, 387
Wiseman P., et al., 2020, MNRAS, 498, 2575
Zampieri L., 2017, in Alsabti A. W., Murdin P., eds, , Handbook of Supernovae. Springer International Publishing, Cham, pp 1 32, doi:10.1007/978-3-319-20794-0_26-1, https://doi.org/10.1007/978-3-319-20794-0_26-1
Zhou R., et al., 2021, MNRAS, 501, 3309

This paper has been typeset from a TEX/LATEX file prepared by the author.